TELKOMNIKA, Vol.11, No.11, November 2013, pp. 6815~6824
e-ISSN: 2087-278X

Control for Wind Power Generation based on Inverse System Theory

Jiyong Zhang*, Guohai Liu
Electrical & Information Engineering Institute, Jiangsu University, Zhenjiang, China
*Corresponding author, e-mail: zjy@yzu.edu.cn

Abstract

Traditional Double-fed Wind Generation systems are based on the vector control method, and it dependents on motor parameters. The performance of the control system will be affected with the parameters changing. This paper proposes a new control method based on inverse system and variable structure sliding mode (VSS) theories, through the inverse system theory, the structure of its state's equation, obtaining the structure of the inverse system, the establishment of Wind Power Generation closed-loop control system is established. The VSS controller, designed with exponential reaching law, can improve the dynamic performance in normal operation range effectively. When the system operates with variable speed constant frequency (VSCF) and the phase voltage drops, the simulations show that the control system can control the DC link voltage steabily, maintain unity power factor, achieve the decoupling of the active and reactive power. And experiments show that the control method used in VSCF wind power system is feasible.

Keywords: *DFIG, inverse system, VSS, VSCF*

1. Introduction

Wind power is relatively cheap and has good prospects for development, is also an inexhaustible energy. Now many countries attach great importance to the utilization of Wind power. In the field of Wind power generation, the system of VSCF is a mainstream, Especially the use of Doubly-fed induction generation is the most promising.

Because wind generators are multivariable nonlinear mechanical and electrical systems with strongly couplings, classical control methods can not meet the requirement of control accuracy and dynamic performance. At present, many systems are based on vector control strategies, in the Grid side, vector control is used based on the grid voltage [1, 2], in rotor side, vector control is used based on the stator flux orientation, so the decoupling between the active and reactive power is achieved. But there are still some problems: (1) The system is sensitive to disturbances and parameters. (2) The control performance of the unit in the DC link voltage and power factor is not satisfied [3, 4].

Inverse system method is a new theory for nonlinear system feedback linearization with clear physical concept and easy to use, has wide application. The literature [5-7] are aimed at some problems in vector control proposes an inverse system method, the analysis and design of Wind Power converter control provides convenience. In this paper, the simulation and experimental results show that the control system has good peformance.

2. Research Method

2.1. The Model of DFIG and Grid Side Converter

2.1.1. The Structure of DFIG Wind Power System

The basic structure of DFIG system is shown in Figure 1. For Doubly-fed machine, the main operation is operating under the sub-synchronous and super synchronous speed condition. The system contains two PWM converters as the grid side and rotor side converters.

Received May 3, 2013; Revised July 19, 2013; Accepted August 4, 2013

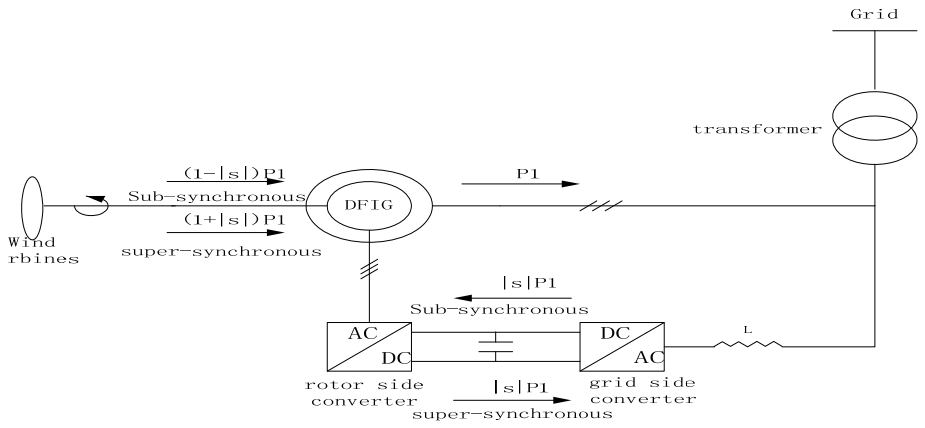

Figure 1. The Basic Structure of DFIG Wind Power Plan

2.1.2. The Mathematical Model of DFIG in Grid Side Converter

VSCF wind power generation system requires Grid side converter controls the DC link voltage steadily, maintains unity power factor, and achieves the decoupling between active and reactive power. In order to achieve high performance of three-phase PWM converter, we should to develop and analyze its mathematical models firstly, and then through the coordinate transformation into the mathematical model of the dq coordinate system [8-13]. Three-phase PWM converter for grid side of the circuit topology is shown in Figure 2.

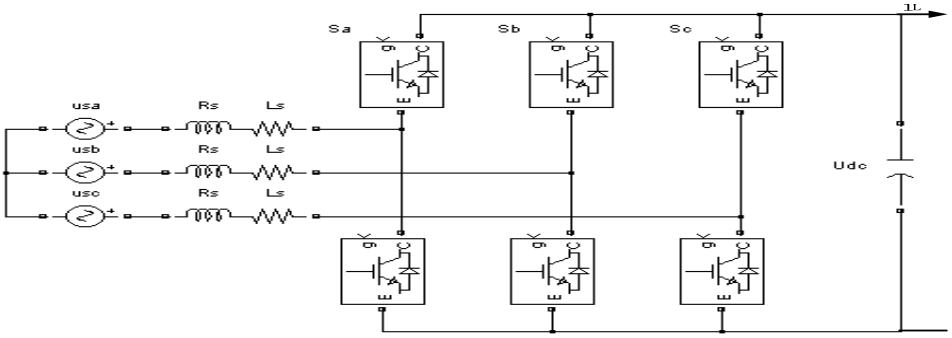

Figure 2. Structure of Gride Side Converter

According to Figure 2, the mathematical model in the abc coordinate system can be written as:

$$\begin{aligned} L_s\frac{di_a}{dt} &= u_{sa} - R_s i_a - (s_a - \frac{s_a + s_b + s_c}{3})U_{dc} \\ L_s\frac{di_b}{dt} &= u_{sb} - R_s i_b - (s_b - \frac{s_a + s_b + s_c}{3})U_{dc} \\ L_s\frac{di_c}{dt} &= u_{sc} - R_s i_c - (s_c - \frac{s_a + s_b + s_c}{3})U_{dc} \\ \frac{du_{dc}}{dt} &= \frac{1}{C}(s_a i_a + s_b i_b + s_c i_c) - \frac{i_L}{C} \end{aligned} \quad (1)$$

Sk is defined as:

$$s_k = \begin{cases} 1 & \text{The top device is on} \\ 0 & \text{The bottom device is on} \end{cases}$$

Three-phase power supply voltage is as follows:

$$\begin{aligned} u_{sa} &= U_m \cos \omega t \\ u_{sb} &= U_m \cos(\omega t - 120^\circ) \\ u_{sc} &= U_m \cos(\omega t + 120^\circ) \end{aligned} \quad (2)$$

Under the principle of coordinate transformation, abc coordinates to dq coordinates transformation's matrix equation for the voltage can be expressed as:

$$C_{3s/2r} = \sqrt{\frac{2}{3}}\begin{bmatrix} \cos\omega t & \cos(\omega t - 120^\circ) & \cos(\omega t + 120^\circ) \\ -\sin\omega t & -\sin(\omega t - 120^\circ) & -\sin(\omega t + 120^\circ) \end{bmatrix} \quad (3)$$

According to Equation (3), the coordinate transformation from abc to dq, the Equation (1), Equation (2) and Equation (3) are combined .It can get the mathematical model of three-phase voltage-type PWM converter in dq coordinate system,

$$\frac{di_d}{dt} = \omega i_q + \frac{u_{sd}}{L_s} - \frac{R_s i_d}{L_s} - \frac{s_d U_{dc}}{L_s} \quad (4)$$

$$\frac{di_q}{dt} = -\omega i_d + \frac{u_{sq}}{L_s} - \frac{R_s i_d}{L_s} - \frac{s_q U_{dc}}{L_s} \quad (5)$$

$$\frac{dU_{dc}}{dt} = \frac{1}{C}(s_d i_d + s_q i_q) - \frac{i_L}{C} \quad (6)$$

In Equation (4), (5) and (6), $u_{sd} = \sqrt{\frac{3}{2}}Um$, $u_{sq} = 0$, S_d , S_q is the equivalent switching function in dq coordinate system.

In the dq coordinates, the voltage and current vectors are expressed as:

$$u_s = u_{sd} + ju_{sq} = u_{sd} \quad (7)$$

$$i = i_d + ji_q \quad (8)$$

Therefore, the complex power input is expressed as:

$$S = u_s * i^* = u_{sd} * (i_d - ji_q) = u_{sd} * i_d - ji_q u_{sd} = P + Q \quad (9)$$

The Equation (9) shows, i_d and i_q control respectively Grid side of the converter's active power and reactive power.

$$P = u_{sd} * i_d \quad (10)$$

$$Q = -u_{sd} * i_q \quad (11)$$

2.2. The Control Structure of Inverse System in Grid Side Converter

The inverse system control is to be achieved by constructing α-order inverse system, the original system is compensated to a linear transitive relation that is a decoupling and pseudo-linear composite system. With the linear decoupling subsystems, it can design the closed-loop controller, which is shown in Figure 3.

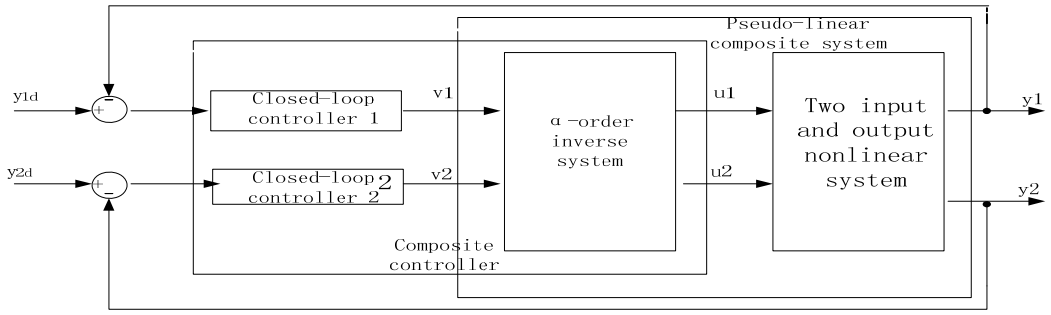

Figure 3. The Controller Formed by α -order Inverse System and Closed-loop Control

According to the derivation, the system state variables can be selected as:

$$[x_1 \quad x_2 \quad x_3]^T = [i_d \quad i_q \quad U_{dc}]^T$$

The output variables can be selected as:

$$[y_1 \quad y_2]^T = [i_d \quad i_q]^T$$

The input variables can be selected as:

$$[u_1 \quad u_2]^T = [s_d \quad s_q]^T$$

The above state variables from the Equation (4) to (6), can be rearranged as follows:

$$\dot{x}_1 = \omega x_2 + \frac{u_{sd}}{L_s} - \frac{R_s x_1}{L_s} - u_1 \frac{x_3}{L_s} \tag{12}$$

$$\dot{x}_2 = -\omega x_1 + \frac{u_{sq}}{L_s} - \frac{R_s x_2}{L_s} - u_2 \frac{x_3}{L_s} \tag{13}$$

$$\dot{x}_3 = \frac{1}{C}(u_1 x_1 - u_2 x_2) - \frac{i_L}{C} \tag{14}$$

From the Equation (12) and (13), u_1 , u_2 can be achieved as:

$$u_1 = \frac{\omega L_s x_2}{x_3} - \frac{R_s x_1}{x_3} + \frac{u_{sd}}{x_3} - \frac{\dot{x}_1 L_s}{x_3} \tag{15}$$

$$u_2 = -\frac{\omega L_s x_1}{x_3} - \frac{R_s x_2}{x_3} + \frac{u_{sq}}{x_3} - \frac{\dot{x}_2 L_s}{x_3} \tag{16}$$

Solve the $\alpha(1,1)$ order intergral inverse system from $\dot{x}_1 = \dot{y}_1 = v_1$, $\dot{x}_2 = \dot{y}_2 = v_2$:

$$u_1 = \frac{\omega L_s x_2}{x_3} - \frac{R_s x_1}{x_3} + \frac{u_{sd}}{x_3} - \frac{v_1 L_s}{x_3} \tag{17}$$

$$u_2 = -\frac{\omega L_s x_1}{x_3} - \frac{R_s x_2}{x_3} + \frac{u_{sq}}{x_3} - \frac{v_2 L_s}{x_3} \tag{18}$$

Three-phase PWM converter control system in Grid side is to keep the current and voltage phase same (Unity power factor), and the DC link voltage steable. According to the above conditions.

When the system is stable:

$$i_q = 0 \qquad U_{dc} = U_{dc}^* \tag{19}$$

$$\dot{i}_q = 0 \qquad \dot{i}_d = 0 \qquad \dot{U}_{dc} = 0 \tag{20}$$

Substitue and simplify the Equation (4)-(6) as follows:

$$S_d U_{dc} = u_{sd} - \frac{R_s P}{u_{sd}} \tag{21}$$

$$S_q U_{dc} = -\omega L_s i_d \tag{22}$$

$$i_d = \frac{U_{dc}^* u_{sd} i_L}{(u_{sd}^2 - R_s P)} \tag{23}$$

When *Rs* is small, it can be ignored, $\dot{i}_d$ steady-state values:

$$\bar{i}_d = \frac{U_{dc}^* i_L}{u_{sd}} \tag{24}$$

In order to eliminate the impact of Rs and the steady-state error of DC link voltage, $\dot{i}_d^*$ can be modified as:

$$i_d^* = k_p(U_{dc}^* - U_{dc}) + ki\int (U_{dc}^* - U_{dc}) + \frac{U_{dc}^* i_L}{u_{sd}} \tag{25}$$

Closed-loop controller can be achieved by the VSS controller. It is designed according to exponential reaching law, can improve the dynamic performance in normal operation range effectively. The sliding surface switching function is designed as follow:

$$S = [S_1, S_2]^T \tag{26}$$

$$\begin{cases} S_1 = e_{i_d} = i_d^* - i_d \\ S_2 = e_{i_q} = i_q^* - i_q \end{cases} \tag{27}$$

Where i_d^* and i_q^* are the grid side reference of active and reactive current, and for the operation of unit power factor, must keep $i_q^* = 0$ .The switching function derivation as bellow:

$$\begin{cases} \dot{S}_1 = \dot{e}_{i_d} = -\dot{i}_d \\ \dot{S}_1 = \dot{e}_{i_q} = -\dot{i}_q \end{cases} \tag{28}$$

The matrix differential equation of switching function derivation is:

$$\dot{S} = F + DU \tag{29}$$

Where U is the matrix of control law, the coefficient matrix are $F = [F_1, F_2]^T$ and D. The control law U is as follows:

$$U = -D^{-1}\begin{bmatrix} F_1 + K_1 S_1 + K_2 sign(S_1) \\ F_2 + K_3 S_2 + K_4 sign(S_2) \end{bmatrix} \quad (30)$$

It shows that the outputs can tracke system input by VSS controller. Then the desired current output can be achieved. The structure of system control is shown in Figure 4:

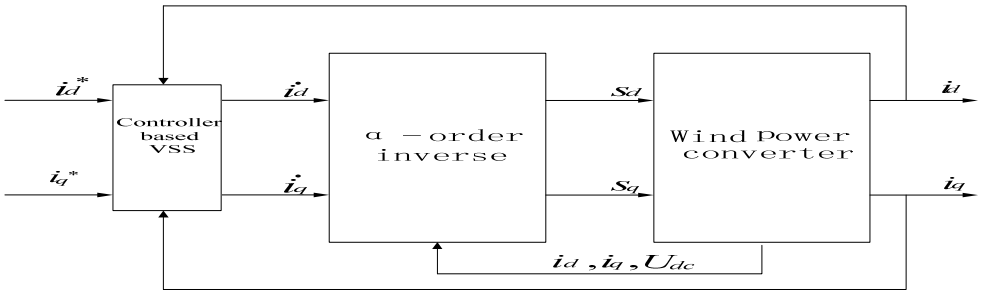

Figure 4. Block Diagram of the Control System

2.3. The Structure of the Control System

In the paper, the structure of the system based on inverse system method is shown in Figure 5:

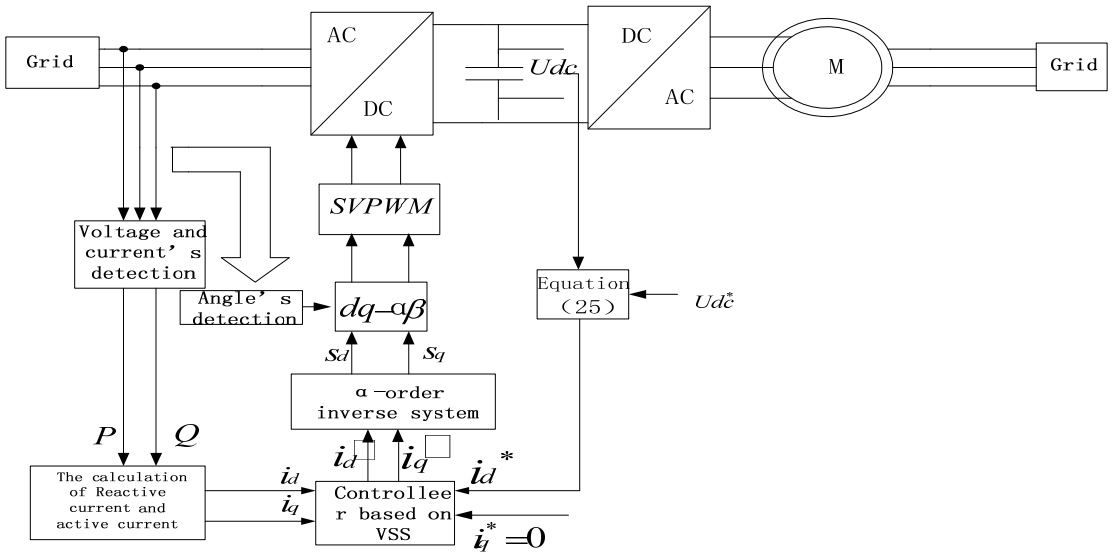

Figure 5. The Structure of the Control System

With the voltage and current detection's operation, through the calculation, the active and reactive power can be achieved. the angle of the left angle of detection can be also achieved. The space vector PWM (SVPWM) is used to control the six bridges to turn on or off. The utilization of the mode keeps the switching frequency of converter bridges constant, to facilitate the design of AC side filter inductance.

3. Results and Analysis

3.1. System simulation

In order to show the high performance of the proposed pseudo-linear inverse system, this paper uses the Matlab/Simulink software to simulate the control system. Simulation parameters are listed as follows: DFIG power rated power 7.5*kw*, stator resistance 0.435Ω, rotor leakage inductance 2*mH*, rotor resistance 0.816Ω, rotor leakage inductance 69.31*mH*, moment of inertia 0.089kg/m^2, voltage in Grid side 690*V*, the DC link voltage 1200*V*, line resistance of Rs = 0.05Ω, line inductance Ls = 6*mH*,the DC link capacitor C = 2200*uf*.

When DFIG operates steabily, the output active power of stator side is sure, according to capturing the maximum power and power balance, when the wind turbine input power changes, the converter power is also changing. If the wind speed reduces to cause that | S | is twice bigger than the original, then the active power | S | P1 from the converter increases to twice.

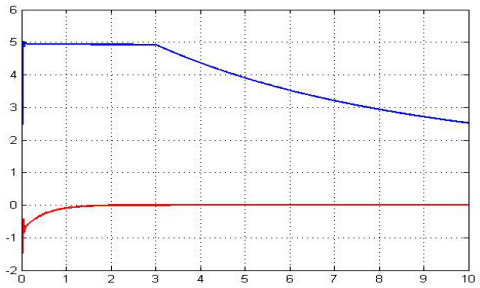

(a) active power under inverse system & VSS control

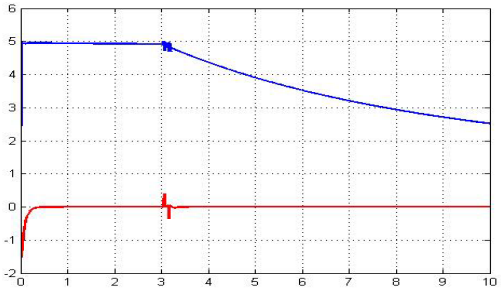

(b) active power under conventional vector control

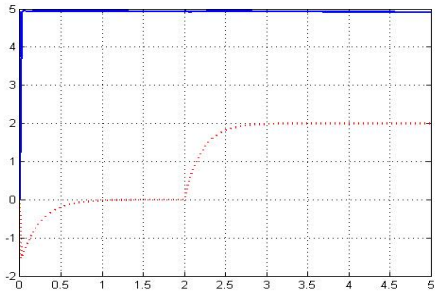

(c) reactive power under inverse system & VSS control

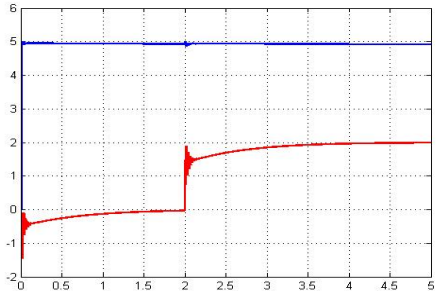

(d) reactive power under conventional vector control

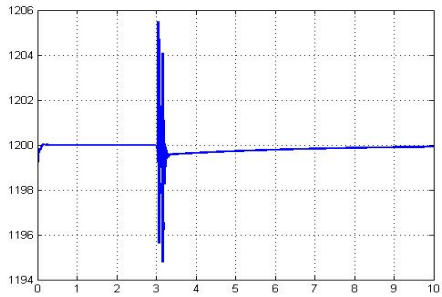

(e) DC voltage under inverse system & VSS control

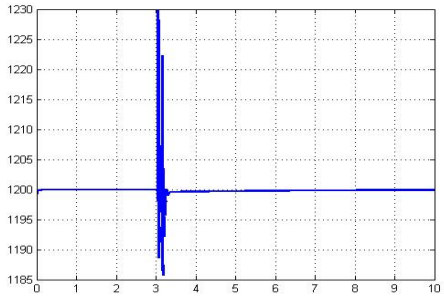

(f) DC voltage under conventional vector control

Figure 6. Active power, reactive power and DC voltage under the inverse system & VSS control and conventional vector control

Figure 6(a), (b) shows that before 3 seconds DFIG is in steady state and the DC link voltage is stable. After 3 seconds wind speed decreases, active power and reactive power are reaching rapidly to the references. From the Figure 6(c), (d), at 2 seconds, the reference of reactive power is increased from 0 to 2Kvar. It can be concluded that the control performance of inverse system and VSS is better than of conventional vector control. Figure 6(e), (f) shows the simulation of the DC link voltage fluctuates, after a period of time the voltage is still maintaining stable, so it is sure that DC link voltage under inverse system and VSS control is more stable.

Figure 7(a), (b), (c) shows the simulation of A phase voltage and current, DC link voltage when A phase voltage drop 20% at 1 seconds, the phase voltage recovers at 1.15 seconds. From the simulation it can be seen that when the voltage drops, the phase current increases, but they are still able to maintain the same phase, The DC link voltage fluctuates, it will be still stable after a period of time. Simulation results show that the control method of inverse system & VSS has better dynamic stability than conventional vector control.

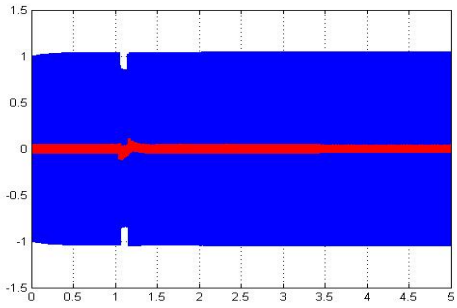

(a) A-phase voltage and phase current

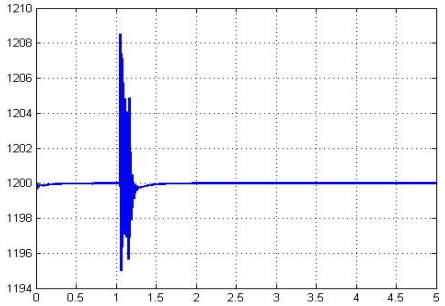

(b) DC voltage under inverse system & VSS control

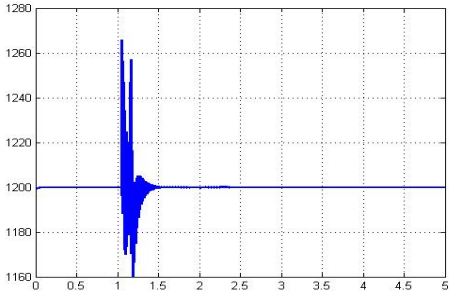

(c) DC voltage under conventional vector control

Figure 7. Results when A-phase Voltage Drops by 20% at 1 seconds

3.2. System Experiment

System experiment parameters are set as follows:

DFIG power rated power 7.5*kw*, voltage rating is 380V, current rating is 20A, speed rating is 750r/min, n_p=4, stator resistance 1.25Ω, stator inductance 9.75*mH*, rotor resistance 0.355Ω, rotor inductance 9.75*mH*, mutual inductance is 67.75mH, inertia of rotation is 0.2Kgm^2, voltage in Grid side 380*V*, the DC link voltage 650*V*, line resistance of Rs = 0.1Ω, line inductance Ls = 2*mH*,the DC link capacitor C = 2200*uf*.

From experimental results, it can be found that the DC voltage was maintained well under subsynchronous and supsynchronous operation. Grid side was keeping unit power factor. From Figure 8(e), (f), the active power and reactive power have been decoupled, the active power and reactive power can be regulated independently.

Experimental results are showed as follows:

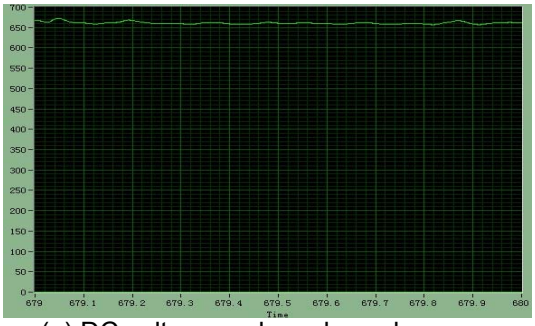
(a) DC voltage under subsynchronous

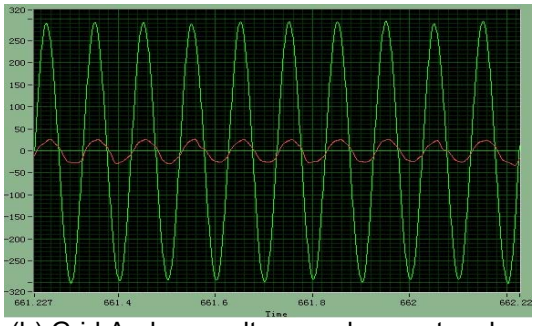
(b) Grid A-phase voltage and current under subsynchronous

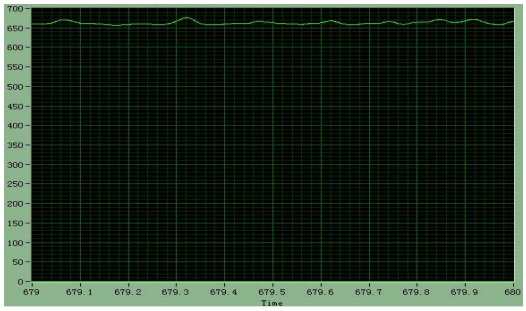
(c) DC voltage under supsynchronous

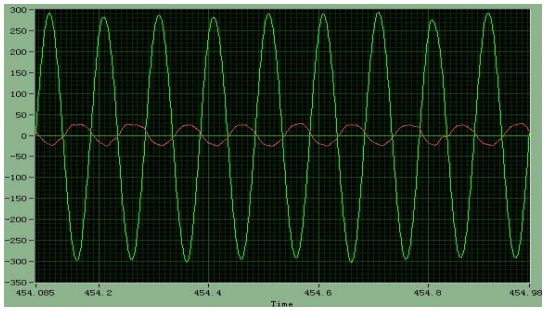
(d) Grid A-phase voltage and current under supsynchronous

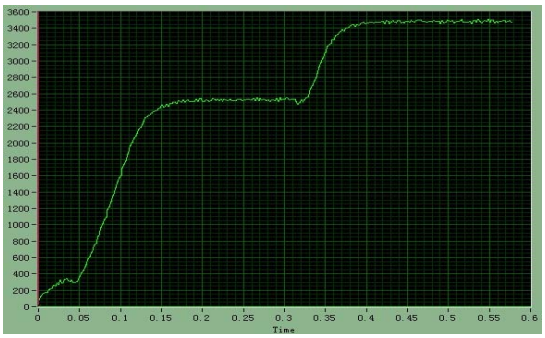
(e) Stator side active power

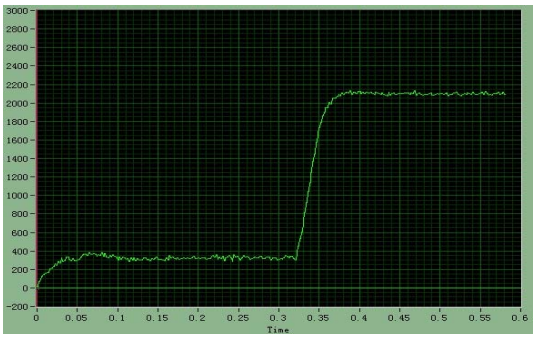
(f) Stator side reactive power

Figure 8. The Experimental Results of DC Voltage, Grid A-phase Voltage & Current, Active Power and Reactive Power

4. Conclusion

In this paper, a pseudo-linear control system is constructed based on the mathematical model of Grid side converter and the inverse system theory. With decoupling dq current, the decoupling of active and reactive power is achieved. Closed loop controller based on VSS can improve the system stability and dynamic performance. By simulation and experiment results, the proposed control method has been verified. And simulation and experimental results show that the proposed control strategy of inverse system and VSS has good performance.

References

[1] Sujith Mohandas, Ashwani Kumar Chandel. Transient Stability Enhancement of the Power System with Wind Generation*. TELKOMNIKA Indonesian Journal of Electrical Engineering.* 2011; 9(2): 267-278.

[2] R Chedid. Intelligent Control for Wind Energy Conversion Systems*. Wind Engineering*. 1998; 22(1): 1-16.

[3] Jie Feng, Huang jin. Novel Modulation Method for Direct Power Control of Three-phase PWM Rectifier. *Power Electronics.* 2006; 40(4): 9-11.
[4] DAI Xianzhong, Liu Guohai, Zhang Xinghua the inversecontrol of AC drive neural network Beijing: Mechanical Industry Press, 2007: 30-45.
[5] Chen Boshi. Automatic control systems of electric drive - motion control system - Edition 3 Beijing: Mechanical Industry Press, 2003: 151-160.
[6] Li Tai, Wang Ben. The control based on inverse system in three-phase PWM rectifier. *Electrical transmission.* 2008; 38 (10):33-38.
[7] Li Chunwen, Feng Yuankun. The inverse control of the multivariable nonlinear system. Beijing: Tsinghua University Press, 1991: 20-26.
[8] Wang Zhaoan, Wang jun. The technology of power electronics. Beijing: Mechanical Industry Press, 2000: 92-95.
[9] Trzynadlowski AM, Legowaki SF. Minimum-loss Vector PWM Strategy for Three-phase Inverters. IEEE Trans. *Power Electron*. 1994; 9(2): 26-34.
[10] Mohanty KB. Input-Output Linearization and Decoupling Control of an Induction Motor Drive. *Journal of the Institution of Engineers*. 2007; 88(2): 45-51.
[11] Trzynadlowski AM, Legowaki SF. Minimum-loss Vector PWM Strategy for Three-phase Inverters. *IEEE Trans.Power Electron*. 1994; 9(2): 26-34.
[12] Sira Ramire H. Nolinear P-I controller design for switchmode DC-to-DC power converters. *IEEE Trans.Circuit Syst.* 1991; 38(4): 410-417.
[13] Long Xian-lin. Influence to Wind Power Farm Line Protection Setting Due to Low Voltage Ride-through. *Inner Mongoi in Electric Power.* 2011; 29(2): 8-12.